Optical-Frequency Transfer over a Single-Span 1840 km Fiber Link

S. Droste,[1,*] F. Ozimek,[2,†] Th. Udem,[1] K. Predehl,[1,∥] T. W. Hänsch,[1,‡] H. Schnatz,[2] G. Grosche,[2] and R. Holzwarth[1,§]

[1]*Max-Planck-Institut für Quantenoptik, Hans-Kopfermann-Strasse 1, 85748 Garching, Germany*
[2]*Physikalisch-Technische Bundesanstalt, Bundesallee 100, 38116 Braunschweig, Germany*
(Received 17 May 2013; published 12 September 2013)

To compare the increasing number of optical frequency standards, highly stable optical signals have to be transferred over continental distances. We demonstrate optical-frequency transfer over a 1840-km underground optical fiber link using a single-span stabilization. The low inherent noise introduced by the fiber allows us to reach short term instabilities expressed as the modified Allan deviation of 2×10^{-15} for a gate time τ of 1 s reaching 4×10^{-19} in just 100 s. We find no systematic offset between the sent and transferred frequencies within the statistical uncertainty of about 3×10^{-19}. The spectral noise distribution of our fiber link at low Fourier frequencies leads to a τ^{-2} slope in the modified Allan deviation, which is also derived theoretically.

DOI: 10.1103/PhysRevLett.111.110801 PACS numbers: 06.20.fb, 06.30.Ft, 42.62.Eh

Modern high-performance frequency standards represent indispensable tools in various fields of research. State-of-the-art optical atomic frequency standards outperform the current cesium based clock standards in both stability and uncertainty [1–4]. They serve as frequency references for tests of the validity of quantum electrodynamics, to verify the constancy of fundamental constants and other experiments that can be performed locally [5–7]. Many applications in fundamental physics, navigation, time keeping, or relativistic geodesy [8–11], however, require the transfer of clock signals between precision measurement laboratories at remote sites. In the field of geodesy, for instance, the transfer of state-of-the-art clock signals allows for the determination of gravitational potential differences where the difference in height of the clock locations can be measured with accuracies in the centimeter range [5]. As optical clocks are considered as candidates for a future redefinition of the second in the International System of Units (SI) [12], the feasibility of high precision remote comparisons between those clocks is a prerequisite. The most common means for transferring stable frequencies to date is based on radiofrequency transfer via satellites, using either the global positioning system (GPS) or a dedicated two-way satellite transfer [13,14]. While these well-established techniques are sufficient for the dissemination of most microwave clock signals, their instability of a few parts in 10^{16} after a measurement time of one day is insufficient to transfer the highly stable signals generated by modern optical clocks. The dissemination capability of these stable optical signals, however, helps to exploit the full potential of optical clocks and opens the path for a variety of experiments.

In recent years several groups around the world have investigated optical fiber links as a possible medium for transferring today's most stable existing frequencies [15–19]. Precision measurement laboratories across Europe are separated by distances up to 2500 km. To compare the increasing number of optical clocks in Europe, stable and accurate frequency transfer over such distances has to be achieved.

In this Letter, we present the coherent transfer of a 194 THz carrier (1542.5 nm) over a 1840-km long fiber link across Germany. A pair of 920-km long dedicated fibers connects the Max-Planck-Institut für Quantenoptik (MPQ) in Garching and the Physikalisch-Technische Bundesanstalt (PTB) in Braunschweig [15]. By connecting the two fiber ends at PTB, we construct a 1840-km link, with sender and receiver being located at MPQ. Between the institutes the fibers are running in parallel in the same cable duct. The whole link includes 20 remotely controllable fiber amplifiers (EDFA) [15] at 11 different locations and two fiber Brillouin amplifiers (FBA) [20] to compensate for more than 420 dB of optical attenuation introduced by the fibers. The fiber link is subject to temperature induced optical path length variations and acoustic noise that produce Doppler frequency shifts on the transmitted signals. Active Doppler cancellation is required to compensate for frequency shifts of up to 20 Hz. In contrast to cascading multiple fiber links, as investigated by Lopez *et al*. [21], we stabilize the whole 1840-km link in a single span. This approach yields a simpler setup, as no intermediate repeaters or stable lasers have to be installed and operated along the link. The critical hardware for stabilization is located at the sender site of the link, which makes it easier to maintain. Those advantages, however, come at the cost of a severely reduced servo bandwidth for the suppression of fiber-induced noise, due to the propagation delay of the light in the fibers. In the case of our link the round-trip time τ_R for the signal is about 18 ms, limiting the servo bandwidth to about 27 Hz. The round-trip time may lead to a somewhat different Doppler shift for the signal at the remote end and the return signal used to cancel the phase noise, thus giving rise to the so called delay-unsuppressed fiber noise. In particular, the Doppler cancellation has no effect on noise at frequencies $f > (1/2\tau_R)$ while for lower frequencies the noise reduction is limited to $\approx (1/3)(\pi f \tau_R)^2$ even for a perfect Doppler cancellation [22] at the sender.

Figure 1 shows a schematic of the fiber link. The linewidth (and thus the laser phase noise) of the cw fiber laser is reduced to approximately 1 Hz by locking it to a high-finesse optical reference cavity [23]. The light of this laser is sent from MPQ to PTB in one of the fibers. At PTB, the optical power of the transmitted light is boosted by amplifiers after which it is sent back to MPQ through the second fiber. Back at MPQ a fraction of the light is retroreflected

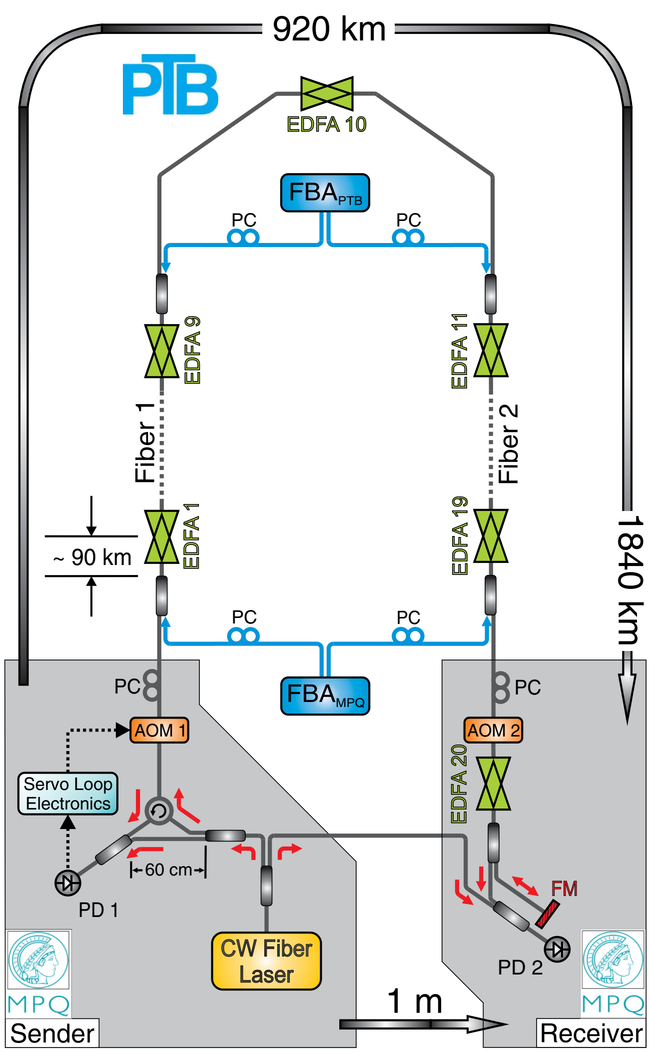

FIG. 1 (color online). Schematic of the optical fiber link. Light of a commercial cw fiber laser locked to an optical cavity is launched into an underground telecommunication fiber at MPQ. After a 1840-km loop the light arrives back at MPQ where a fraction of it is retroreflected. The round-trip light is used to derive an error signal for a servo loop with AOM 1 as the actuator. EDFA: erbium-doped fiber amplifier, FBA: fiber Brillouin amplifier, AOM: acousto-optic modulator, PC: polarization controller, FM: Faraday mirror, PD: photo diode.

with orthogonal polarization by a Faraday mirror. When the retroreflected light eventually reaches its origin it has been amplified 40 times by EDFAs and 4 times by FBAs and a beat signal is generated between the retroreflected light and the sent light (PD 1 in Fig. 1). Mixing this signal with a fixed frequency reference generates a phase error signal that serves as an input for a servo loop that drives the frequency of an acousto-optic modulator (AOM 1 in Fig. 1). This Doppler cancellation compensates for fluctuations of the optical path length due to acoustics and temperature variations along the fiber [24]. The Doppler cancellation setup can be understood as an interferometer with a short (≈ 60 cm) reference arm and a long ($\approx 2 \times 1840$-km) arm. The short arm is not part of the Doppler cancellation servo loop and needs to be well isolated from the lab environment. At the receiver end of the link another AOM (AOM 2 in Fig. 1) introduces a constant frequency shift in order to distinguish the retroreflected light from spurious back reflections that occur at connectors and splices along the link. The link performance is determined by characterizing a rf beat signal that contains the relevant out of loop information and is generated from the nonreflected portion of the transferred light and the sent light (PD 2 in Fig. 1).

The beat notes on PD 1 and PD 2 are tracked [25] and recorded with dead time free frequency counters [26] with a maximum sample rate of 1 kHz. To prevent cycle-slip events (loss of phase coherence) from entering the data analysis we use a redundant counting scheme [27]. For this purpose the beat notes at PD 1 and PD 2 are each fed to two frequency counters at the same time. With a gate time of 1 s, we discard all data points where the two counters counting identical signals disagree by more than 0.2 Hz, indicating a cycle slip. As the beat note on PD 1 is stabilized by the Doppler cancellation to 20 MHz we also discard data points where this in-loop signal deviates by more than 5 Hz from the nominal value at a gate time of 1 s. This threshold was adapted to 25 times the standard deviation of the frequency fluctuations.

In Fig. 2 the instability of the transferred frequency of the free-running link as well as that of the stabilized link, both expressed as the overlapping Allan deviation (ADEV) [28], is shown. Data with gate times larger than the recording gate time are obtained by computing an unweighted average of nonoverlapping adjacent and dead time free data points. This corresponds to the so called Π-type evaluation [29] by which we obtain a value for the ADEV of 1.3×10^{-13} in 1 s for the stabilized link. This agrees well with the $L^{3/2}$-scaling law [22] for a link with length L when we compare it with our previous results of 3×10^{-15} [24], 2×10^{-14} [20], and 4×10^{-14} [15] for fiber links of lengths 146 km, 480 km, and 920 km, respectively.

In addition, we use counters operating in the so called overlapping Λ mode [29,30]. In contrast to the Π mode,

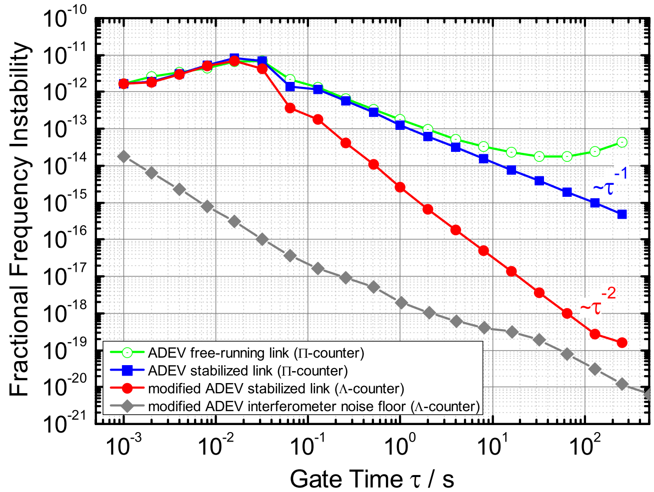

FIG. 2 (color online). Fractional frequency instability of the 1840-km free-running fiber link (open circles) and the stabilized link (squares) derived from a nonaveraging (Π-type) frequency counter and expressed as the ADEV. To obtain a significantly shorter measurement time and to distinguish between white phase, flicker phase, and other noise types [29], averaging (overlapping Λ-type) frequency counters may be used for which the modified ADEV (filled circles) measures the instability. Also shown is the measured noise floor of the interferometer (diamonds). The transferred frequency is subject to phase noise at measurement times of up to 20 ms that cannot be compensated for by the control loop due to the signal delay in the fiber.

these counters sample the phase of the input signal with a rate much larger than the gate time τ. With such an oversampling, noise is effectively averaged out, so that more accurate data are obtained in a shorter time. With these counters three overlapping adjacent counter readings are combined to another overlapping Λ-type data point with twice the gate time by computing the average value with relative weights (1,2,1). The instability derived from overlapping Λ-type data corresponds to the modified ADEV [29] (red filled circles in Fig. 2). We analyzed the longest cycle-slip free interval to calculate the modified ADEV. The residual instability is 2.7×10^{-15} in 1 s and falls off as τ^{-2}. The reason for this fast reduction lies in the spectral noise distribution of our fiber link at frequencies below 20 Hz as will be discussed below. For a gate time of 100 s, the instability reaches 4×10^{-19}, which surpasses the requirement for an optical clock comparison today by more than one order of magnitude. Using modern overlapping Λ-type counters and generating the modified ADEV, the fiber link's frequency instability can be evaluated in only a few hundred seconds. The smooth τ^{-2} slope in the modified ADEV could not be seen in our previous results on a 920-km link [15] as we had to use counters at both fiber ends that could not be perfectly synchronized. In combination with a residual laser drift, this leads to a deviation from the τ^{-2} slope. The three main contributions that might lead to a floor in the instability are (1) undetected cycle slips, (2) the noise of the cw transfer laser, and (3) the noise floor of our interferometer. We estimated these contributions individually in detail and obtained very similar upper limits of about 1×10^{-20} for each of them with the current setup.

The transferred frequency could be subject to a systematic and stable offset, for example due to the large propagation delay, which would not be revealed in the instability analysis. Therefore, the accuracy has to be checked independently. After measuring the transferred frequency with a Λ-type frequency counter with a gate time of 1 s over a period of three days, we calculate unweighted mean values for all cycle-slip free 100 s long segments. We use this Π-type evaluation here to avoid overweighting the center parts of long data sets with the triangular weighting. Of all 1 s data points in Fig. 3, 98.5% were validated, and two thirds made it into the 100 s sets. Due to randomly appearing cycle slips, these data contain dead time. Figure 3 shows the difference between the sent and the transferred frequency for a gate time of 1 s and the selected 100 s data subsets. The 1367 data points have an arithmetic mean of $-2.7\ \mu$Hz (-0.14×10^{-19}) and a standard deviation of 1.9 mHz (1×10^{-17}). The latter is a factor 100 smaller than the modified ADEV at $\tau = 1$ s as expected for this Π-type evaluation. The statistical fractional frequency uncertainty is 50 μHz (2.6×10^{-19}) and the transferred frequency shows no deviation from the sent frequency within this uncertainty.

Complementary to the time-domain approach, a wide spread frequency domain characterization of phase instability is the power spectral density (PSD) of phase fluctuations $S_\phi(f) = |\tilde{\phi}(2\pi f)|^2$ with the Fourier transform normalized to the measurement time of the phase $\phi(t)$

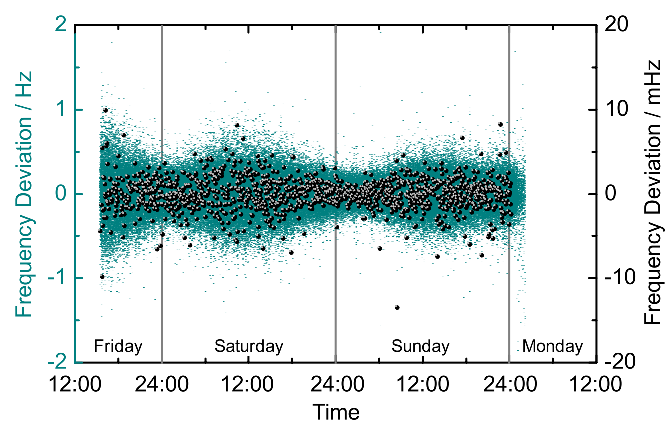

FIG. 3 (color online). Three-day frequency comparison between sent and transferred frequency after 1840 km. Data were taken with a dead-time free Λ-type frequency counter with 1-s gate time (green data points). The arithmetic means of all cycle-slip free 100 s intervals have been computed. From the resulting 1367 data points (black dots, right frequency axis, enlarged scale) a fractional difference between sent and transferred frequency of $(-0.14 \pm 2.6) \times 10^{-19}$ is calculated.

between the sent and transferred optical waves. The phase noise PSD has been measured for the stabilized fiber link and for the free-running link, where no Doppler cancellation was applied (see Fig. 4). The free-running link features a distinct broad maximum around 15 Hz similar to Refs. [20,24], above which the noise rolls off quickly. We attribute this maximum to building and ground vibrations. The Doppler cancellation system suppresses the noise within its servo bandwidth, i.e., below 27 Hz. From Fig. 4 it can be seen that the measured noise suppression is close to the theoretical limit for delay-limited noise suppression, derived in Ref. [22]. With the Doppler cancellation system active the noise increases with Fourier frequency up to $f \approx 20$ Hz.

In the literature, the phase noise PSD is usually parametrized as [31,32]

$$S_\phi(f) = \sum_{\alpha=-2}^{2} h_\alpha f^{\alpha-2} \tag{1}$$

with the constant h_α as a measure of the noise level. This means that, in a phase noise PSD as it is shown in Fig. 4, only noise that falls off with frequency as $f^{-4}, f^{-3}, \ldots$ or frequency independent noise (f^0) is covered by this model. The phase noise PSD of our stabilized fiber link, however, rises with frequency up to about 20 Hz so that we have to extend the model by additional higher order terms $h_\alpha f^{\alpha-2}$ for $\alpha > 2$.

The modified Allan variance can be calculated from phase fluctuations $S_\phi(f)$ using the equation [28,33]

$$\mathrm{mod}\,\sigma_y^2(\tau) = \frac{2}{\nu_{\mathrm{opt}}^2} \int_0^\infty S_\phi(f) \frac{\sin^6(\pi f \tau)}{(\pi n \tau)^2 \sin^2(\frac{\pi \tau f}{n})} df \tag{2}$$

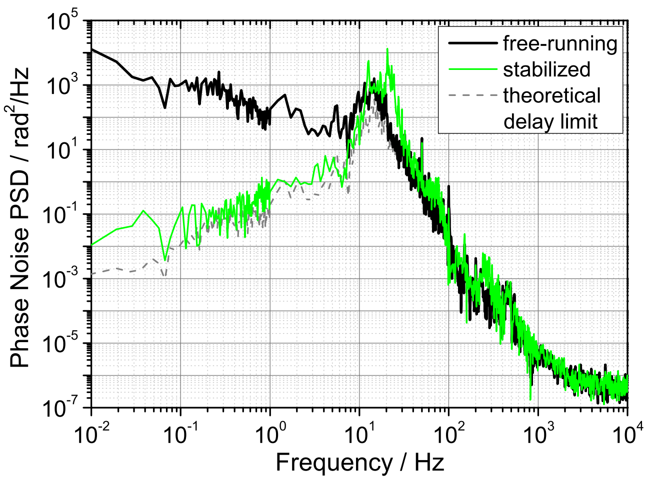

FIG. 4 (color online). Phase noise power spectral density $S_\phi(f)$ of the free-running (thick black line) and the stabilized (green line) 1840-km link. The servo bump around 27 Hz is in agreement with the bandwidth limit due to the propagation delay. Also shown is the Doppler noise suppression limit [22] (dashed gray line).

with the number of samples n used to determine $S_\phi(f)$ (n drops out as it goes to infinity) and the optical carrier frequency ν_{opt}. This integral can be calculated analytically and is found in the literature for the five noise types mentioned above [29,33]. However, analytical solutions also exist for the case of $\alpha > 2$. A noise spectrum of the form $S_\phi(f) = h_3 f$ for instance leads to

$$\mathrm{mod}\,\sigma_y^2(\tau) = \frac{10\gamma + \ln(48) + 10\ln(\pi f_h \tau)}{\nu_{\mathrm{opt}}^2 16\pi^4} h_3 \tau^{-4} \tag{3}$$

with the Euler's constant $\gamma = 0.577\ldots$, assuming a sharp cutoff frequency f_h. The modified ADEV $\mathrm{mod}\sigma_y(\tau)$ then shows a slope of τ^{-2}. Similar expressions can be derived for noise spectra with $\alpha > 3$—all showing the τ^{-2} dependency. The spectral noise distribution of our fiber link therefore leads to the observed τ^{-2} dependency of the modified Allan deviation. Using Eq. (2) with the measured phase noise PSD data (see Fig. 4) yields the measured modified ADEV (see Fig. 2) within the measurement uncertainty.

For the Doppler cancellation we used a standard proportional-integral (PI) controller without any phase advance circuitry that would be capable of dealing with the large signal delay of about 18 ms. A specially designed loop filter [34] could reduce the influence of the servo bump and thus decrease the overall phase noise of the stabilized link. The transferred carrier frequency exhibits a rms phase jitter of almost 160 radians for the stabilized link. Despite these large phase fluctuations, continuous tracking of the phase is accomplished by using tracking oscillators and digital phase detectors.

In summary, we demonstrated that highly stable optical frequencies can be transferred over nearly 2000 km with a series of bidirectional optical amplifiers and without the need of intermediate signal repeater stations. The attenuation introduced by the fibers is compensated by a series of remotely controllable amplifiers. In this work we daisy chained 20 EDFAs and two FBAs, while the round-trip light used for the stabilization passes the whole link twice. Thus, we could show that even after almost 3700 km of fiber and 44 amplification stages, we still achieve signal-to-noise ratios of the heterodyne beat signals on the order of 40 dB in a 10 kHz resolution bandwidth. By using the modified ADEV for the instability analysis we could demonstrate an unprecedented fast reduction with the gate time proportional to τ^{-2} that enabled a substantial reduction in measurement time.

This work was supported by the European Metrology Research Programme (EMRP) under SIB-02 NEAT-FT. The EMRP is jointly funded by the EMRP participating countries within EURAMET and the European Union. We thank S. M. F. Raupach for establishing the frequency scheme as well as for implementation and maintenance of the hardware at PTB. We thank J. Alnis and Th. Legero for setting up the ultrastable reference cavities, O. Terra for his work on the fiber Brillouin amplifiers, and the members of Deutsches Forschungsnetz in Berlin, Leipzig, and Erlangen, Germany, as well as Gasline GmbH for a fruitful collaboration. We also thank the excellence cluster QUEST for financial support. T. W. H. acknowledges support by the Max Planck Foundation.

*To whom all correspondence should be addressed. stefan.droste@mpq.mpg.de

†Also at Institute of Experimental Physics, Faculty of Physics, University of Warsaw, ul. Hoza 69, 00-681 Warszawa, Poland.

‡Also at Ludwig-Maximilians Universität, Schellingstrasse 4, 80799 München, Germany.

§Also at Menlo Systems GmbH, Am Klopferspitz 19a, 82152 Martinsried, Germany.

‖Present address: LNE-SYRTE Observatoire de Paris, 61 Av. de l'Observatoire 75014 Paris, France.

[1] H. Katori, Nat. Photonics **5**, 203 (2011).

[2] M. D. Swallows, M. Bishof, Y. Lin, S. Blatt, M. J. Martin, A. M. Rey, and J. Ye, Science **331**, 1043 (2011).

[3] N. Huntemann, M. Okhapkin, B. Lipphardt, S. Weyers, C. Tamm, and E. Peik, Phys. Rev. Lett. **108**, 090801 (2012).

[4] J. A. Sherman, N. D. Lemke, N. Hinkley, M. Pizzocaro, R. W. Fox, A. D. Ludlow, and C. W. Oates, Phys. Rev. Lett. **108**, 153002 (2012).

[5] C. W. Chou, D. B. Hume, J. C. J. Koelemeij, D. J. Wineland, and T. Rosenband, Phys. Rev. Lett. **104**, 070802 (2010).

[6] A. Shelkovnikov, R. J. Butcher, C. Chardonnet, and A. Amy-Klein, Phys. Rev. Lett. **100**, 150801 (2008).

[7] C. G. Parthey, A. Matveev, J. Alnis, B. Bernhardt, A. Beyer, R. Holzwarth, A. Maistrou, R. Pohl, K. Predehl, T. Udem, T. Wilken, N. Kolachevsky, M. Abgrall, D. Rovera, C. Salomon, P. Laurent, and T. W. Hänsch, Phys. Rev. Lett. **107**, 203001 (2011).

[8] A. Matveev, C. G. Parthey, K. Predehl, J. Alnis, A. Beyer, R. Holzwarth, T. Udem, T. Wilken, N. Kolachevsky, M. Abgrall, D. Rovera, C. Salomon, P. Laurent, G. Grosche, O. Terra, T. Legero, H. Schnatz, S. Weyers, B. Altschul, and T. W. Hänsch, Phys. Rev. Lett. **110**, 230801 (2013).

[9] C. W. Chou, D. B. Hume, T. Rosenband, and D. J. Wineland, Science **329**, 1630 (2010).

[10] S. Schiller *et al.*, Exp. Astron. **23**, 573 (2009).

[11] J. Müller, M. Soffel, and S. A. Klioner, J. Geodes. **82**, 133 (2008).

[12] P. Gill, Phil. Trans. R. Soc. A **369**, 4109 (2011).

[13] A. Bauch, J. Achkar, S. Bize, D. Calonico, R. Dach, R. Hlavać, L. Lorini, T. Parker, G. Petit, D. Piester, K. Szymaniec, and P. Uhrich, Metrologia **43**, 109 (2006).

[14] M. Fujieda, T. Gotoh, F. Nakagawa, R. Tabuchi, M. Aida, and J. Amagai, IEEE Trans. Ultrason. Ferroelectr. Freq. Control **59**, 2625 (2012).

[15] K. Predehl, G. Grosche, S. M. F. Raupach, S. Droste, O. Terra, J. Alnis, T. Legero, T. W. Hänsch, T. Udem, R. Holzwarth, and H. Schnatz, Science **336**, 441 (2012).

[16] O. Lopez, A. Haboucha, B. Chanteau, C. Chardonnet, A. Amy-Klein, and G. Santarelli, Opt. Express **20**, 23 518 (2012).

[17] M. Fujieda, M. Kumagai, S. Nagano, A. Yamaguchi, H. Hachisu, and T. Ido, Opt. Express **19**, 16 498 (2011).

[18] G. Marra, R. Slavík, H. S. Margolis, S. N. Lea, P. Petropoulos, D. J. Richardson, and P. Gill, Opt. Lett. **36**, 511 (2011).

[19] L. Sliwczynski, P. Krehlik, L. Buczek, and M. Lipinski, IEEE Trans. Instrum. Meas. **61**, 2573 (2012).

[20] O. Terra, G. Grosche, and H. Schnatz, Opt. Express **18**, 16 102 (2010).

[21] O. Lopez, A. Haboucha, F. Kéfélian, H. Jiang, B. Chanteau, V. Roncin, C. Chardonnet, A. Amy-Klein, and G. Santarelli, Opt. Express **18**, 16 849 (2010).

[22] P. A. Williams, W. C. Swann, and N. R. Newbury, J. Opt. Soc. Am. B **25**, 1284 (2008).

[23] J. Alnis, A. Matveev, N. Kolachevsky, T. Udem, and T. W. Hänsch, Phys. Rev. A **77** (2008).

[24] G. Grosche, O. Terra, K. Predehl, R. Holzwarth, B. Lipphardt, F. Vogt, U. Sterr, and H. Schnatz, Opt. Lett. **34**, 2270 (2009).

[25] L.-S. Ma, P. Jungner, J. Ye, and J. L. Hall, Opt. Lett. **19**, 1777 (1994).

[26] G. Kramer and W. Klische, in *Proceedings of the 2001 IEEE International Frequency Control Symposium and PDA Exhibition, Seattle, Washington, 2001* (IEEE, New York, 2001), pp. 144–151.

[27] T. Udem, J. Reichert, T. W. Hänsch, and M. Kourogi, Opt. Lett. **23**, 1387 (1998).

[28] W. Riley, *Handbook of Frequency Stability Analysis*, NIST Special Publication 1065 (National Institute of Standards and Technology, Gaithersburg, MD, 2008).

[29] S. Dawkins, J. McFerran, and A. Luiten, IEEE Trans. Ultrason. Ferroelectr. Freq. Control **54**, 918 (2007).

[30] E. Rubiola, Rev. Sci. Instrum. **76**, 054703 (2005).

[31] J. A. Barnes, A. R. Chi, L. S. Cutler, D. J. Healey, D. B. Leeson, T. E. McGunigal, J. A. Mullen, W. L. Smith, R. L. Sydnor, R. F. C. Vessot, and G. M. R. Winkler, IEEE Trans. Instrum. Meas. **IM-20**, 105 (1971).

[32] J. Rutman and F. Walls, Proc. IEEE **79**, 952 (1991).

[33] L. Bernier, in *41st Annual Symposium on Frequency Control. 1987* (IEEE, New York, 1987), pp. 116–121.

[34] B. S. Sheard, M. B. Gray, and D. E. McClelland, Appl. Opt. **45**, 8491 (2006).